Chromosoma (2011) 120:245–254
DOI 10.1007/s00412-010-0307-4

RESEARCH ARTICLE

Atomic force microscope imaging of chromatin assembled in *Xenopus laevis* egg extract

Hongxia Fu · Benjamin S. Freedman · Chwee Teck Lim · Rebecca Heald · Jie Yan

Received: 25 October 2010 / Revised: 14 December 2010 / Accepted: 16 December 2010 / Published online: 11 January 2011

Abstract Gaps persist in our understanding of chromatin lower- and higher-order structures. *Xenopus* egg extracts provide a way to study essential chromatin components which are difficult to manipulate in living cells, but nanoscale imaging of chromatin assembled in extracts poses a challenge. We describe a method for preparing chromatin assembled in extracts for atomic force microscopy (AFM) utilizing restriction enzyme digestion followed by transferring to a mica surface. Using this method, we find that buffer dilution of the chromatin assembly extract or incubation of chromatin in solutions of low ionic strength results in loosely compacted chromatin fibers that are prone to unraveling into naked DNA. We also describe a method for direct AFM imaging of chromatin which does not utilize restriction enzymes and reveals higher-order fibers of varying widths. Due to the capability of controlling chromatin assembly conditions, we believe these methods have broad potential for studying physiologically relevant chromatin structures.

Communicated by E. Nigg

H. Fu · C. T. Lim · J. Yan
Mechanobiology Institute, National University of Singapore, Singapore, Singapore

H. Fu · J. Yan
Department of Physics, National University of Singapore, Singapore, Singapore

B. S. Freedman · R. Heald (✉)
Department of Molecular and Cell Biology, University of California, Berkeley, CA, USA
e-mail: bheald@calmail.berkeley.edu

C. T. Lim
Division of Bioengineering and Department of Mechanical Engineering, National University of Singapore, Singapore, Singapore

J. Yan (✉)
Centre for Bioimaging Sciences, National University of Singapore, Singapore, Singapore
e-mail: phyyj@nus.edu.sg

Introduction

Eukaryotic genomic DNA is packaged with histones into chromatin, which is the template upon which essential cellular processes such as gene expression and DNA replication occur. The fundamental subunit of chromatin is the nucleosome, which is composed of 147 bp DNA wrapped 1.7 times in a left-handed superhelix around a core histone octamer (Davey et al. 2002; Luger et al. 1997; Noll 1974). Repeating nucleosome arrays are compacted by histone H1 into fibers of 30 nm width (Huynh et al. 2005; Thoma and Koller 1977), which may be further compacted into higher-order structures by scaffolding proteins (Horowitz-Scherer and Woodcock 2006; Paulson and Laemmli 1977). In vitro, chromatin folds intrinsically, depending on ionic strength, forming nucleosome-on-a-string structures at low ionic strength (~5 mM monovalent ions) and 30-nm fibers at higher concentrations (Huynh et al. 2005; Thoma and Koller 1977). Various techniques such as electron microscopy have been utilized to provide nanometer-scale resolution of purified reconstituted chromatin; however, it remains unclear how lower-order chromatin structures are folded and organized into the much larger cellular structures of interphase nuclei and mitotic chromosomes (Fakan 2004; Horowitz-Scherer and Woodcock 2006; Horowitz et al. 1994; Kireeva et al.

2004; McDowall et al. 1986; Woodcock 1994). For instance, despite decades of research, it is still not clear whether chromatin takes the form of "30-nm" fiber in vivo or whether a proteinaceous scaffold lies at the core of mitotic chromosomes (Eltsov et al. 2008; Kireeva et al. 2004). One roadblock to answering such questions is that existing techniques rely largely on chromatin purified from living cells, for which genetic manipulation is difficult and frequently lethal. Experiments are therefore typically limited to localization studies on wild-type chromatin or the biochemical manipulation of chromatin purified away from the in vivo context in which it normally functions.

Cellular extracts from *Xenopus laevis* oocytes and eggs or *Drosophila melanogaster* embryos can remodel naked DNA into nucleosome arrays similar to those in living cells but can also be manipulated biochemically to investigate specific components (Becker 2007; Hirano and Mitchison 1991; Laskey et al. 1977; Lusser and Kadonaga 2004; Ruberti and Worcel 1986). Thus, a factor which is essential in living cells can be immunodepleted from egg extract without activating apoptotic pathways, and its effect on de novo chromatin assembly from naked DNA can be determined by comparison to a wild-type control extract. Egg extracts have been used to elucidate the roles of essential proteins such as the condensin complex and histone H1 in complex macromolecular structures such as interphase nuclei and mitotic chromosomes (Maresca et al. 2005; Wignall et al. 2003). Chromatin assembled in interphase egg extract associates with several known non-nucleosomal chromatin structural components including cohesin, SWI/SNF, and HP-1, and features heterochromatin histone methylation marks, similar to chromatin in living cells (Fischle et al. 2005; Losada et al. 1998; MacCallum et al. 2002; Maresca et al. 2005). However, until recently, there have been few investigations of extract-assembled chromatin at the single-molecule or ultrastructural level (Bennink et al. 2001; Ladoux et al. 2000; Yan et al. 2007). Such studies might be especially useful for understanding chromatin higher-order structure, which has been difficult to visualize in extracts and many other systems (Woodcock and Ghosh 2010). In an effort to characterize single-molecule dynamics of physiological chromatin, we recently reported that naked, random-sequence DNA could be folded by 20-fold-diluted egg extract against forces of a few piconewtons (pN) and could be unfolded by applying forces ≥4 pN. The folding process was dependent on ATP hydrolysis, while unfolding had a characteristic step size of ~147 bp, suggesting that nucleosomes were successfully assembled along the DNA (Yan et al. 2007). The structures of the folded DNA in the extracts were not inspected by microscopy; however, a previous report suggests the formation of nucleosome-like structures under similar conditions (Ladoux et al. 2000). Here, we describe techniques to routinely prepare chromatin in egg extracts of sufficient purity and stability for atomic force microscope (AFM) imaging. We use these methods to investigate the impact of ionic strength and extract dilution on chromatin structure and to provide evidence of hierarchical folding in higher-order chromatin structures. These methods make it possible to study the function of essential proteins in physiologically relevant, de novo chromatin assembly at the scale of lower-order chromatin structure.

Materials and methods

X. laevis egg extract

Demembranated sperm nuclei and cytostatic factor (CSF)-arrested low-speed *X. laevis* egg extracts were prepared as described by Maresca and Heald (2006) and Murray (1991). To generate low-speed interphase-arrested egg extracts, CSF extract was supplemented with 50 μg/ml cycloheximide and 0.05 volumes of $CaCl_2$ solution (10 mM $CaCl_2$ in XB buffer: 100 mM KCl, 1 mM $MgCl_2$, 0.1 mM $CaCl_2$, 10 mM K–HEPES pH 7.7, 50 mM sucrose) and incubated at room temperature for 45 min. High-speed extracts were prepared by centrifuging low-speed interphase-arrested extracts at 200,000×*g* and flash-freezing the cytosol fraction as described (Maresca and Heald 2006).

Chromatin assembly in *Xenopus* egg extract and enzyme digestion

Xenopus egg extract was diluted two-, 20-, or 100-fold with XB2 (XB buffer plus an additional 1 mM $MgCl_2$) or HEPES/KCl buffer (50 mM HEPES pH 7.7, 50 mM KCl), supplemented with energy mix (3.75 mM creatine phosphate, 0.05 mM Na_2-ATP, 0.5 mM $MgCl_2$). No obvious differences were observed between these two buffers in the morphology of the resulting chromatin. For ionic strength experiments, two other low salt buffers were used: 10 mM HEPES (pH 7.7), 50 mM sucrose, 1 mM KCl, and 0.2 mM $MgCl_2$, or, alternatively, 10 mM HEPES (pH 7.7), 50 mM sucrose. Fifty microliters of egg extract was applied to a single lambda DNA-coated streptavidin surface at room temperature (24°C) for 1 h in conditions of 60% relative humidity (Fig. 1). After chromatin assembly, the streptavidin surface was washed five times with 200 μl extract dilution buffer to remove most of the adherent egg extract. For the direct imaging method, chromatin was optionally fixed at this point with 1% formaldehyde in XB2 for 15 min before proceeding to the deoinized water wash. For the enzyme digestion method, restriction enzymes were applied at this point to the chromatin-coated surface for 1 h

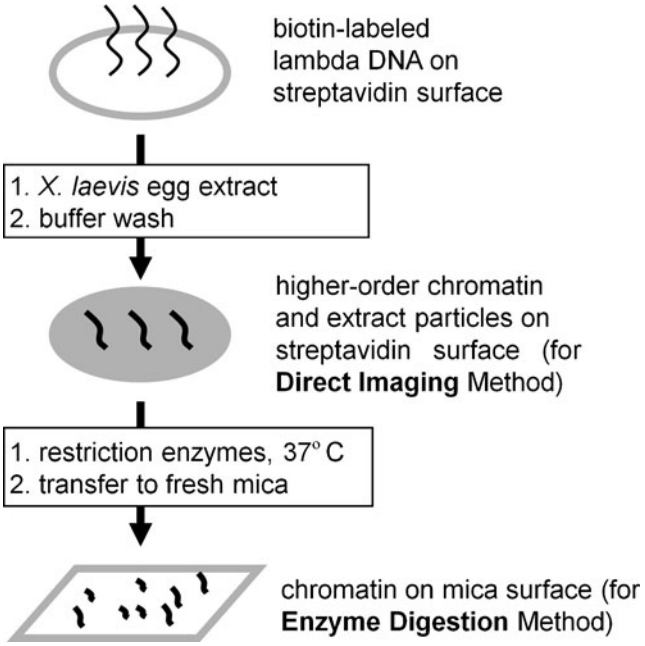

Fig. 1 Schematic of described methodology. A DNA-coated surface is incubated with extract to assemble chromatin, which may be directly imaged for higher-order structures (Direct Imaging Method) or subjected to restriction endonuclease digestion and transferred to fresh mica for visualization of lower-order structures (Enzyme Digestion Method)

(Asc I) or 5 min (Alu I) at 37°C. Since the digestion efficiency of Asc I on chromatin was very low, the digestion buffer was changed to its optimum buffer, NEBuffer 4 (20 mM Tris–acetate, 50 mM potassium acetate, 10 mM magnesium acetate, 1 mM dithiothreitol, pH 7.9; New England Biolabs). Enzyme-digested chromatin in solution was diluted 50-fold to reach low salt concentrations of 1 mM K^+ and 0.2 mM Mg^{2+}. To study the effects of ionic strength, Alu I was applied in low salt buffers instead of its original digestion buffer. Enzyme-digested chromatin was removed and incubated for 30 min on a 0.1% glutaraldehyde mica surface reported to better maintain intact nucleosome structures (Wang et al. 2002). For both the direct imaging and enzyme digestion methods, the mica surface was flushed quickly by deionized water (Millipore) and dried by nitrogen prior to imaging.

Chromatin prepared from live cell nuclei

Hela cells were cultured in Dulbecco's Modified Eagle Medium (DMEM) with 5% FBS in culture dishes and collected by trypsinization. The cells were re-suspended in 10 mM $MgCl_2$, 250 mM sucrose, 0.2 mM phenylmethanesulfonylfluoride (PMSF) (nuclei washing buffer) with 1% Triton X-100 and broken down using shear stress by passing through a 23-gauge needle for about 20 times (Cui and Bustamante 2000; Hameed et al. 2009). The supernatant was removed from the sample by centrifugation. The pelleted nuclei were washed by nuclei washing buffer until clean and stored in XB2 buffer. The nuclei were then unfolded in deoinized water for 30 min to get the unfolded chromatin structures for AFM imaging.

AFM imaging

AFM imaging was performed by AC-mode in air with 60% humidity using Molecular Imaging 5500 AFM (Molecular Imaging, Agilent Technologies). The AFM probe used in all the measurements is silicon AFM probe (Taq300, Budget Sensors). In order to estimate the tip-induced width increase in width measurement, we imaged lambda-phage DNA (Fermentas) on 0.1% glutaraldehyde mica surface using three different AFM probes. Based on statistics from more than 30 line-scans for ten different DNA molecules, the DNA was measured to have a half-maximum-height–width of 11.8± 0.8 nm and a height of 0.7±0.1 nm. Considering that the realistic DNA width is around 2 nm, this result suggests that there is an about 10-nm tip-induced width increase. This tip-induced width increase was subtracted from all the measured values of chromatin and DNA. To estimate the width of nucleosomes in chromatin fibers reconstituted from pure histone octamers or assembled in *Xenopus* egg extracts, line-scans for at least 20 nucleosomes in each type of chromatin fiber were used to estimate the average width and the standard deviation. Finally, more than 100 line-scans for the higher-order chromatin obtained in the direct AFM imaging method under fixed condition were used to measure the width and standard deviation. The images in TIFF format were prepared by freeware Gwyddion.

Two kinds of surfaces used in chromatin imaging are glutaraldehyde-coated mica improved from the protocol described in Wang et al. (2002) and streptavidin-coated mica or glass surface. The streptavidin-coated surface was prepared by the following standard procedure: (1) cleaned glass or mica surface was first silanized by APTES (Sigma) followed by coating with glutaraldehyde (Sigma), (2) 0.02 mg/ml streptavidin (Sigma) in 1× phosphate-buffered saline (PBS) was incubated on the above surface for 8 h at 24°C, (3) the streptavidin-coated surface was passivated with 0.5 M ethanolamine (Sigma) for 1 h at 24°C and then stored in 10 mg/ml bovine serum albumin (BSA; Sigma) at 4°C. Before use, the streptavidin-coated surface was rinsed with 5 ml 1× PBS to remove the excess BSA.

To attach DNA to the streptavidin-coated surface, one end of lambda-phage DNA (Fermentas) was ligated to a biotinylated oligo (Sigma) with T4 DNA ligase (New England Biolabs). Fifty microliters of such DNA (9 ng/μl) was incubated on a ~1-cm^2 streptavidin-coated glass surface at 24°C for 30 min. The surface was then washed for three times using buffer solution. Reconstituted 12-mer

nucleosome arrays were the generous gift of Assistant Professor CA Davey (Nanyang Technological University).

Results

Egg extract contaminants pose a challenge to AFM chromatin imaging

The high concentration of proteins in *Xenopus* egg extract allows for physiological chromatin assembly from naked DNA, but also poses a challenge for ultrastructural imaging. We first attempted to image chromatin directly in undiluted egg extract; however, the abundance of macromolecular contaminants rendered the extract impossible to image even before any DNA was added (Fig. 2a). We next attempted to isolate chromatin by a limiting dilution method similar to one reported previously (Ladoux et al. 2000), but found that the egg extract had to be diluted more than 100,000 times in order to have a clean surface for chromatin imaging (Fig. 2b–d). Such drastic overdilution makes it difficult to use the minimum ratio of ~25 μl extract/μg DNA required for efficient chromatin assembly (Laskey et al. 1977; Ruberti and Worcel 1986) and is likely to damage or precipitate extract activities. Blocking the mica-imaging surface with milk or BSA prior to chromatin assembly did not reduce the heavy extract background, while sedimentation of chromatin through a sucrose-cushion failed to completely eliminate extract contaminants and also resulted in significant losses in yield (data not shown). We, therefore, turned to an affinity purification protocol in which chromatin is assembled in situ from lambda DNA tethered to a solid support. In the past, we and others have used lambda DNA-coated beads for biochemical and nuclease analysis of chromatin assembled in egg extracts (Becker 2007; Sandaltzopoulos and Becker 1999; Yan et al. 2007). This protocol has a high yield, which is important for biochemical analysis, and when we began our imaging experiments, our first inclination was to use this same protocol for AFM imaging. However, it quickly became clear that the approach, while useful for biochemistry, was not suitable for AFM because of the tendency of the DNA to cross-link, fragmentation of the beads upon manipulation, and retention of adsorbed cytoplasm by the beads even after many washes (data not shown). These are not major problems for biochemical analysis, which relies on chemical specificity, but they present difficulties for AFM imaging and necessitated the development of more delicate methods which emphasize quality over quantity. In our preferred method described here, DNA tethered to a mica surface was assembled directly into chromatin, washed, and then subjected to direct imaging for higher-order structures or enzyme digestion for examination of lower-order structures (Fig. 1).

Direct AFM imaging method for higher-order chromatin structures

For the direct imaging method, biotinylated lambda DNA tethered to a streptavidin-coated surface was incubated with extract for 1 h to assemble chromatin, washed, and then directly imaged on the same surface by AFM without enzymatic digestion. This procedure yielded long, thin

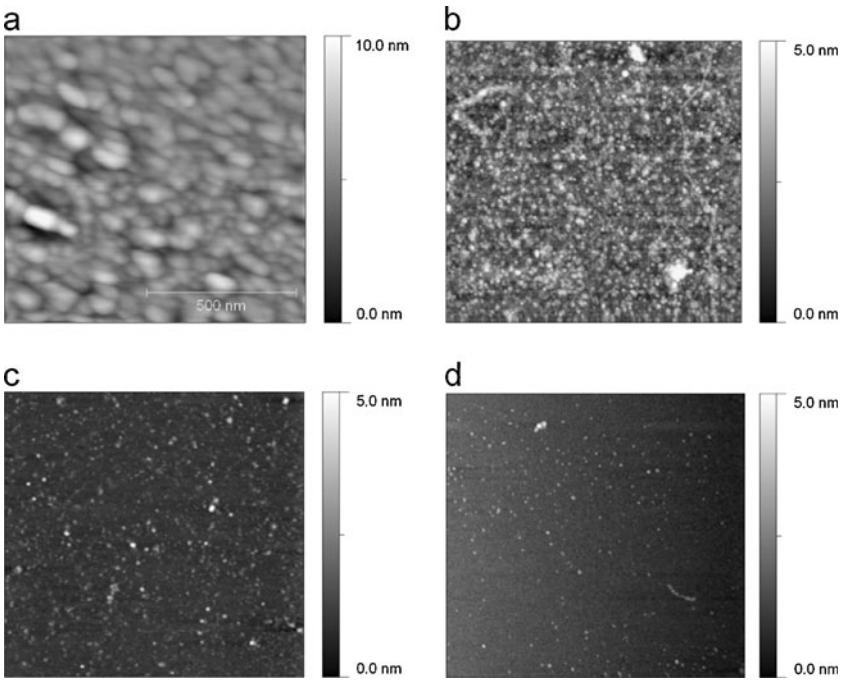

Fig. 2 *Xenopus* egg extract poses a challenge for AFM. AFM images on 0.1% glutaraldehyde mica in air of pure egg extract subjected to **a** no dilution with buffer, **b** 100-fold dilution, **c** 10,000-fold dilution, and **d** 100,000-fold dilution. No DNA was added to these samples. All the image sizes are 1,000 nm× 1,000 nm. *Scale bar* is shown in **a** and applied to all the other images in this figure. Heights are coded from *black to white*

fibers ~10 nm in width from the DNA-coated surface, but no structures were observed when a control surface lacking DNA was substituted (Fig. 3a–b). Although the roughness of the streptavidin surface made it difficult to resolve individual nucleosomes, this method was nevertheless useful for studying higher-order chromatin structures. To control for changes to the chromatin that might occur during the water wash, chromatin was fixed with 1% formaldehyde prior to washing with deionized water, yielding fibers of widths ranging from ~10–120 nm (Fig. 3c), with an average of 64 nm and a standard deviation of 28 nm based on more than 100 line-scans for these higher-order structures. The height of fixed fibers was greater than unfixed ones, and the thinnest fixed-chromatin fibers were similar in width to the ~10-nm fibers observed in the unfixed sample (Fig. 3b). Occasionally, fixed fibers appeared to split into two ~twofold thinner fibers and then re-merge (Fig. 3c). These results are consistent with a model of higher-order folding in which thin chromatin fibers are bundled lengthwise into thicker fibers, which can be disrupted by washes with deionized water. However, since formaldehyde also crosslinks chromatin fibers, it is unclear to what extent fixation preserves the native structure of chromatin.

In order to see how these higher-order folding is similar to in vivo chromatin organization, we compared them with chromatin directly isolated from Hela cell nuclei (see "Materials and methods" for details of nuclei chromatin isolation). Chromatin structures isolated from nuclei were very large. We unfolded them using deoinized water to get smaller structures that were comparable in size to those obtained in *Xenopus* egg extract. We find that the higher-order structures from Hela cell nuclei are similar to those visualized using our method in the egg extract (Fig. 3d, compare to Fig. 3b–c). Water unfolding also resulted in simpler nucleosome arrays (Fig. 3e).

Enzyme digestion method for imaging of nucleosome arrays

Although the direct imaging method was useful for imaging higher-order structures of chromatin, the roughness of the streptavidin chromatin assembly surface and the adherence of egg extract contaminants made it difficult to resolve

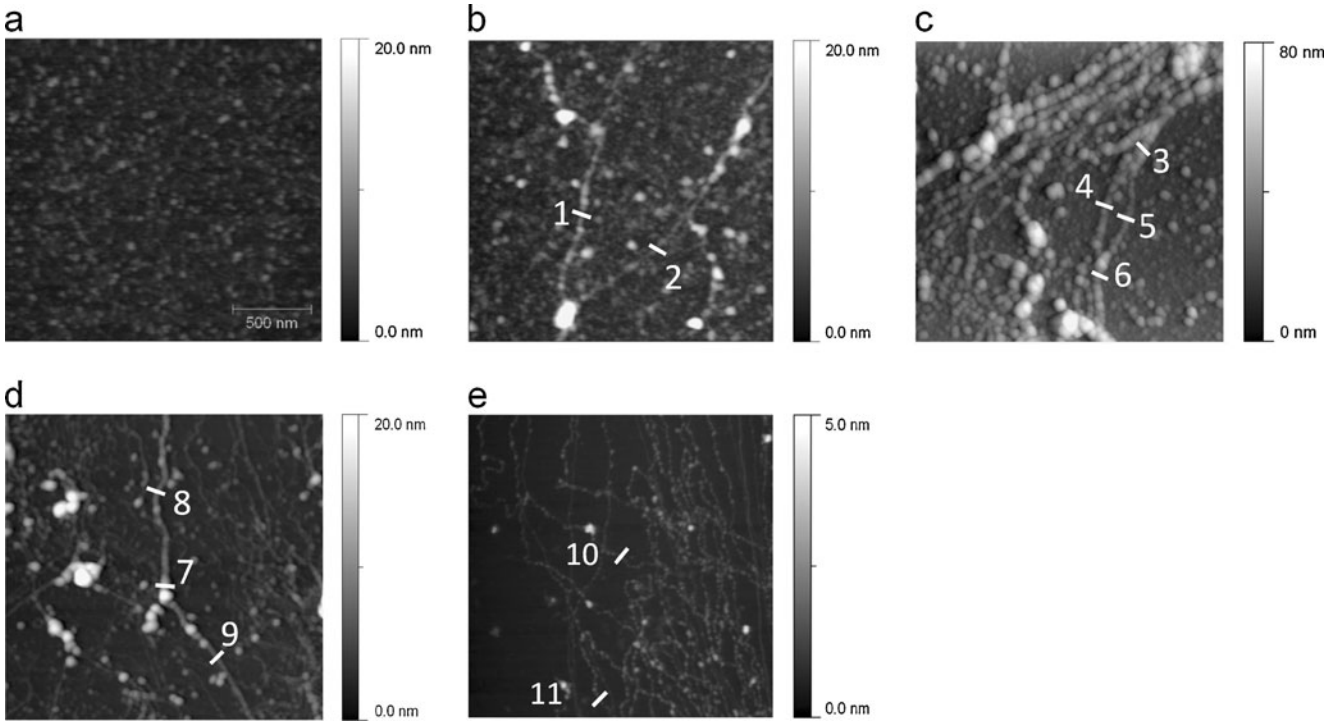

Fig. 3 Direct imaging method for AFM of higher-order structures. AFM images of chromatin assembled from lambda-phage DNA in *Xenopus laevis* egg extract on streptavidin-coated surface and imaged directly on the same surface. **a** The control surface without DNA, treated with extract and then washed with deionized water. No large structures are observed. **b** DNA-coated surface treated with extract and then washed with deionized water without fixation. Widths of fiber sections in different areas are labeled in white: (*1*) 13 nm and (*2*) 8.3 nm. **c** Sample as in **b** but fixed with 1% formaldehyde before washing with deionized water. Widths of sections labeled in *white*: (*3*) 37.4 nm, (*4*) 20.7 nm, (*5*) 13.4 nm, (*6*) 37.2 nm. **d**, **e** Chromatin isolated from Hela cell and unfolded in deionized water without fixation. Widths of sections labeled in *white*: (*7*) 34.3 nm, (*8*) 25.6 nm, (*9*) 29.2 nm, (*10*) 14.7 nm, (*11*) 12.1 nm. All the image sizes are 2,000 nm×2,000 nm. *Scale bar* is shown in **(a)** and applies to all the other images in this figure. Heights are coded from *black to white*

individual nucleosomes in situ. To better visualize lower-order chromatin structures, we treated chromatin fibers in buffer with the restriction enzyme Asc I, which has only two cutting sites in lambda DNA (releasing two fragments of ~13 and ~32 kbp from the DNA-coated surface), and then transferred the released fragments to a clean glutaraldehyde-coated mica surface. When this protocol was performed on a lambda DNA-coated substrate not treated with egg extract, naked DNA strands were released, whereas when it was performed on a substrate lacking DNA but treated with extract, no structures were released, indicating that this method successfully overcame the obstacle of background signal from extract contaminants (Fig. 4a–b). When performed on affixed lambda DNA incubated with 20-fold-diluted egg extract, which in magnetic tweezers experiments causes the stepwise compaction of naked DNA (Yan et al. 2007), large structures were released, portions of which appeared to be unfolded and resembled reconstituted beads-on-a-string nucleosome arrays (Fig. 4c–d). The width and height of the "beads" structure on these chromatin structures appeared similar to the reconstituted 12-nucleosome arrays deposited onto the same type of mica (Fig. 4e) in terms of the size of the "beads" in the "beads-on-a-string" structure between Fig. 4c–d and Fig. 4e. The "beads" in Fig. 4c–d have a width of 8.4±2.9 nm and a height of 1.9±0.2 nm, while those in Fig. 4e have a width of 7.9±2.8 nm and a height of 3.0±0.2 nm. Both values were after subtraction of 10-nm tip-induced width increase. These results are similar to those reported by others of the measurements of 17.6± 2.2 nm in width that includes an ~5.8-nm tip-induced width increase implied by their DNA width measurement of 7.8± 0.2 nm, and 2.8±0.3 nm height for reconstituted nucleosomes on similar mica surfaces (Wang et al. 2002). To demonstrate how the widths of DNA and nucleosome were measured, three representative line-scan profiles are shown in Fig. 4f.

Effect of egg extract dilution on chromatin

Many biochemistry and single-molecule manipulation experiments have studied the structure and properties of

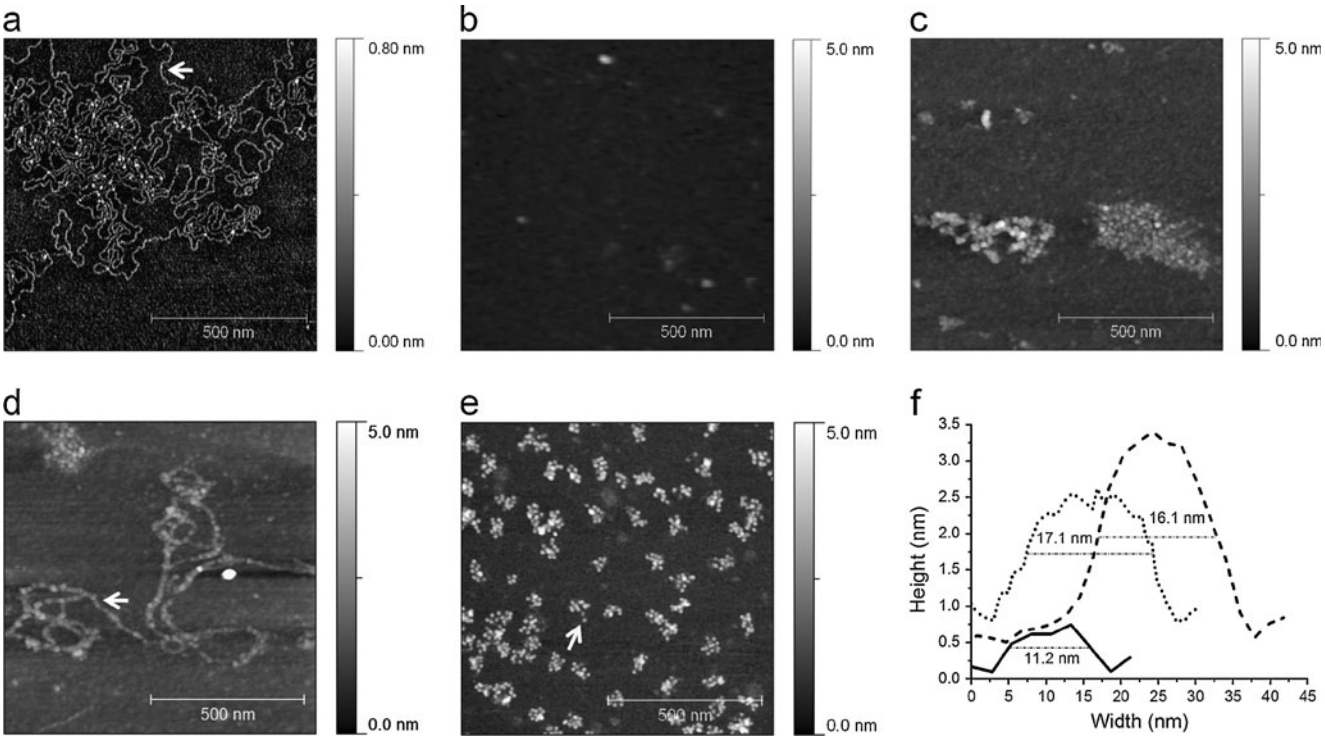

Fig. 4 Enzyme digestion method for AFM of lower-order structures. AFM images of Asc I restriction enzyme digestion products from **a** DNA-coated surface not treated with extract, **b** the control surface without DNA treated with 20-fold-diluted egg extract and then washed with deionized water, and **c**, **d** DNA-coated surface treated with egg extract and washed with deionized water without fixation. **e** Reconstituted 12-mer nucleosome arrays. **f** Representative line-scan profiles for DNA in **a** (*solid line*), a nucleosome in **d** (*dotted line*), and a nucleosome in **e** (*dash line*). The scan locations are indicated by the *arrowheads*. The half-maximum-height-widths before subtracting the tip-induced width increase are indicated by the respective *dashed lines* and the values. The final buffer is 1 mM HEPES (pH 7.7), 1 mM KCl and 0.2 mM $MgCl_2$. Sample **a** was imaged on 0.1% APTES mica in air and **b–e** on 0.1% glutaraldehyde mica in air. Image sizes are 1,000 nm×1,000 nm. *Scale bar* is shown in each picture. Heights are coded from *black to white*. The size of the "beads" in the nucleosome arrays assembled in *Xenopus* egg extract (**c–d**) was measured to be 8.4± 2.9 nm, similar to 7.9±2.8 nm that was measured for the reconstituted ones (**e**)

chromatin assembled in cellular extracts (Ladoux et al. 2000; Ruberti and Worcel 1986; Yan et al. 2007). Frequently, in these experiments, the chromatin assembly extracts were diluted ten- or 20-fold in buffer before their application to the DNA template, but it is not known how dilution of cellular extract affects the chromatin assembly and conformation. To investigate this, we incubated naked DNA with two-, 20-, or 100-fold-diluted high-speed egg extract and examined the resulting chromatin structure by AFM. To better visualize chromatin in the twofold-diluted condition, we determined digestion conditions for Alu I, which is more efficient than Asc I and recognizes more than 100 restriction cleavage sites on lambda-phage DNA. As expected, many more chromatin fragments of smaller size were released after digestion with Alu I compared to Asc I (Fig. 5a). For all the samples, we maintained the minimum ratio of egg extract to DNA (~25 μl original egg extract: 1 μg DNA) for the chromatin assembly reaction—only the dilution factor differed between conditions. Although chromatin-like structures were apparent in all conditions, the fibers assembled in 20- and 100-fold-diluted extracts were of lesser height and were mixed with strands of naked DNA (Fig. 5a–c).

Effect of ionic strength on chromatin

The intrinsic folding of chromatin is expected to depend on the ionic strength of the surrounding buffer (Thoma et al. 1979; Zheng et al. 2005). To test whether fibers obtained using our protocol shared this property, three solutions of decreasing ionic strength were investigated: (1) XB2 buffer [10 mM HEPES (pH 7.7), 50 mM sucrose, 100 mM KCl, 0.1 mM $CaCl_2$ and 2 mM $MgCl_2$], (2) 10 mM HEPES (pH 7.7), 50 mM sucrose, 1 mM KCl and 0.2 mM $MgCl_2$, and (3) 10 mM HEPES (pH 7.7), 50 mM sucrose. Alu I was added into each solution to digest the chromatin assembled on streptavidin-coated surface. The dimensions of chromatin fragments assembled in XB2 buffer (Fig. 6a) and in 10 mM HEPES (pH 7.7), 50 mM sucrose, 1 mM KCl and 0.2 mM $MgCl_2$ (Fig. 6b) are similar to those observed in Fig. 5a. However, in zero-salt buffer (10 mM HEPES (pH 7.7), 50 mM sucrose), nucleosome fibers were unstable and dissociated into small particles or naked DNA (Fig. 6c). These behaviors are consistent with chromatin-containing histone H1, such as the chromatin fragments released from enzyme-digested nuclei, which tend to stay condensed even in low salt buffer but may also rapidly unravel in such buffers if not fixed immediately (Thoma and Koller 1977; Thoma et al. 1979).

Discussion

The methods described here allow rapid, high-yield isolation of chromatin structures assembled in egg extracts for high resolution AFM imaging. The specific association of chromatin proteins with DNA and their assembly into nucleosomes using *Xenopus* egg extracts has been extensively shown by many groups using diverse techniques including MNase digestion and single-DNA stretching experiments (Almouzni and Wolffe 1993; Becker 2007; Yan et al. 2007). While good methods have been published for biochemical analysis of chromatin assembled in extracts (Becker 2007; Sandaltzopoulos and Becker 1999; Yan et al. 2007), the same methods do not work well for AFM imaging, which necessitated the innovation of the protocols presented here. The imaging protocols that are the focus of our paper are based on the same principle of solid-phase immobilization as the existing biochemical methods; however, they have been optimized for minimization of cross-linked chromatin structures and reduced background. Yield is not as high as for lambda DNA-coated beads;

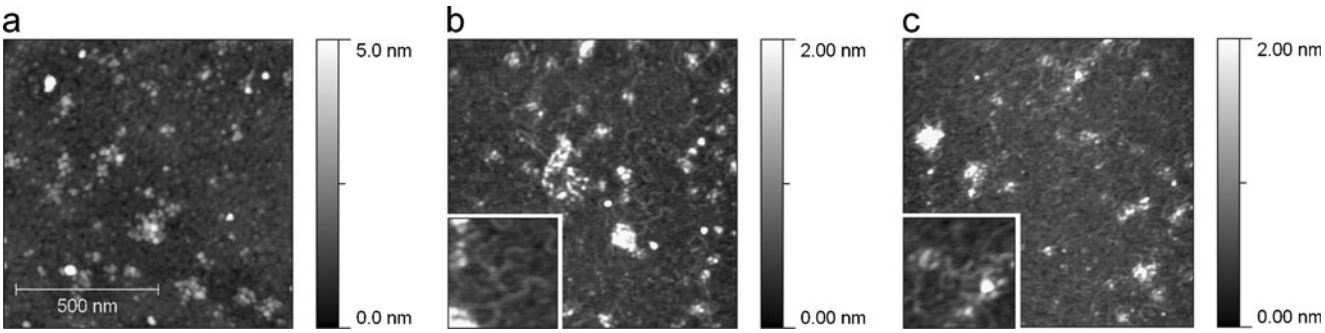

Fig. 5 Diluted extracts produce mixed chromatin and DNA structures. AFM images of chromatin assembled from lambda-phage DNA in **a** two-, **b** 20-, and **c** 100-fold-diluted egg extract digested with restriction enzyme Alu I in XB2 buffer. The final solution is XB2 buffer. *Insets* show strands of naked DNA strands in 20- and 100-fold-diluted samples, which were not visible in the twofold-diluted condition. Chromatin samples are imaged on 0.1% glutaraldehyde mica in air. All the image sizes are 1,000×1,000 nm, but the height scale has been adjusted for the twofold-diluted sample due to the thickness of the sample in that condition. The *scale bar* is shown in **(a)** and applies to all the other images in this figure. Heights are coded from *black to white*

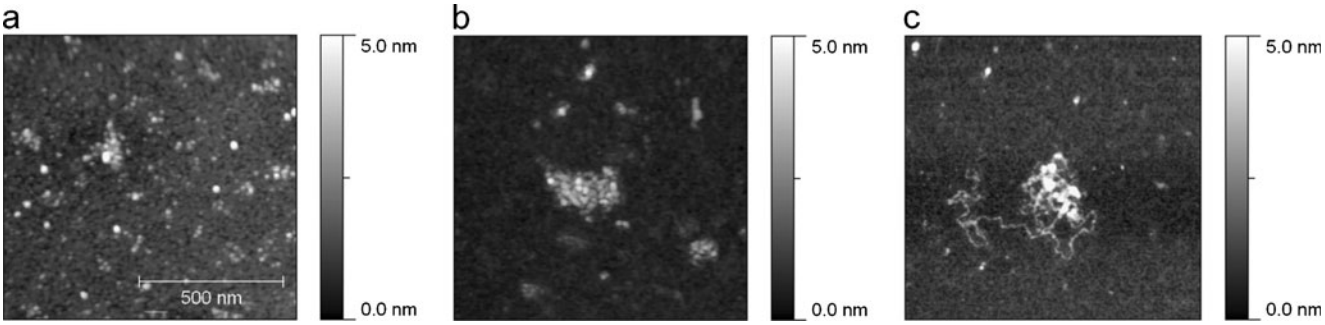

Fig. 6 Low ionic strength destabilizes chromatin. **a–c** AFM images of chromatin assembled from lambda-phage DNA in twofold-diluted egg extract in XB2 buffer and digested with restriction enzyme Alu I. The final buffer is **a** XB2 buffer, **b** 10 mM HEPES (pH 7.7), 50 mM sucrose, 1 mM KCl, and 0.2 mM $MgCl_2$, and **c** 10 mM HEPES (pH 7.7), 50 mM sucrose. Samples are imaged on 0.1% glutaraldehyde mica in air. All the image sizes are 1,000×1,000 nm. The *scale bar* is shown in **(a)** and applies to all the other images in this figure. Heights are coded from *black to white*

nevertheless, it is more than enough for reliable ultrastructural imaging, and it is not difficult to find good fields for AFM imaging. We have demonstrated the use of these methods by investigating the conformational response of the chromatin structures to salt concentration and the dilution of the extracts. The methods are sensitive enough to detect the response of chromatin organization to salt: at lower salt concentrations, the chromatin became more extended. Without salt, exposed DNA could even be seen.

Because AFM lacks chemical specificity, it was important to confirm that the structures imaged were indeed derived from DNA. To distinguish true chromatin structures from egg extract contaminants, we coupled our experiments with careful negative controls in which no DNA was added and compared our putative chromatin fibers to purified HeLa cell chromatin as well as reconstituted nucleosome arrays. Interestingly, while chromatin assembled in twofold-diluted extracts were the most compact, sharp, and stable, chromatin assembled in 20- and 100-fold-diluted extracts resulted in mixed population of chromatin-like fibers and exposed DNA. Previous single-molecule experiments using chromatin assembled in egg extracts were performed at significant degrees of dilution (Bennink et al. 2001; Ladoux et al. 2000; Yan et al. 2007), while our results suggest that attention should be paid to the dilution of the egg extracts in chromatin assembly.

Although individual nucleosomes were clearly seen in the chromatin fragments obtained by enzymatic digestion Fig. 6a–b (also Fig. 4c and Fig. 5a), most of these did not appear as extended nucleosome-on-a-string structures but rather as condensed nucleosome arrays. These are likely to be higher-order structures containing histone H1, which is abundant in extracts and incorporated into extract-assembled chromatin (Maresca et al. 2005). Interestingly, these fibers appear larger and less ordered than chromatin reconstituted from very large DNA molecules containing many regularly spaced tandem nucleosome-positioning DNA sequences, which showed an unexpectedly compact 30-nm fiber (Robinson et al. 2006). Since DNA length and ionic strength was comparable between these two systems and linker histone was present in both, the most likely explanation for this discrepancy is that chromatin fibers assembled in extracts differ significantly from reconstituted chromatin fibers with respect to composition and/or organization. Extracts contain many chromatin-binding proteins not present in simple reconstituted arrays, such as topoisomerases and cohesins, as well as enzymatic activities which can modify histones post-translationally to change their binding affinities. In addition, it has recently been observed that *Xenopus* egg extracts dramatically increase the dynamics of histone H1, resulting in weaker binding of somatic H1 subtypes to sperm chromatin in cytoplasm versus buffer (Freedman et al. 2010). Cytoplasm might therefore promote the assembly of higher-order structures which are actually less compact than the maximal compaction which can be obtained in purified systems, either through the incorporation of additional chromatin-binding proteins or the modulation of core or linker histone affinities for DNA.

Although the intrinsic folding of lower-order structures such as beads-on-a-string nucleosomes is relatively well established, it remains unclear to what extent these intrinsic mechanisms are responsible for the assembly of higher-order chromatin structures observed in vivo, such as nuclei or mitotic chromosomes (Horowitz-Scherer and Woodcock 2006). In the interphase extracts we are using in this paper, lambda DNA or sperm nuclei are remodeled into smoother, puffier structures rather than the sharper, more ragged structures observed in mitotic extracts (Hirano and Mitchison 1991). In these extracts as in other systems, higher-order chromatin structures are thought to be present during interphase but have been difficult to directly visualize. The presence of such structures in egg extracts can be inferred from two sources: (1) nuclei remodeled in extracts have a diameter of ~10 μm, similar to that of nuclei in vivo and

representing a greater level of compaction than could be achieved with nucleosomes alone and (2) chromatin assembled in interphase egg extract associates with several known non-nucleosomal chromatin structural components such as cohesin and HP-1 and features post-translational modifications characteristic of compact heterochromatin (Fischle et al. 2005; Losada et al. 1998; MacCallum et al. 2002; Maresca et al. 2005). Importantly, the techniques described here enable nanoscale visualization of not only nuclease-digested lower-order structures, but also the higher-order structures from which they are derived. These higher-order fibers are nevertheless much smaller than whole chromosomes, with a maximum width of ~90–120 nm [approximately the size of a chromonema fiber (Kireeva et al. 2004)] and can therefore still be traced by AFM imaging. The direct imaging method presented in our manuscript adds to the evidence that higher-order structures form in interphase egg extracts (Fig. 3b–c), while the enzyme digestion method demonstrates that these structures are indeed composed of lower-order chromatin subunits (Fig. 4c–d). In addition, conformational similarity between these chromatin structures to those isolated from Hela cell nuclei (Fig. 3d–e) suggests that these higher-order structures resemble those present in living cells. A more systematic comparison of these higher- and lower-order chromatin structures by AFM, perhaps using a variety of DNA templates as starting material, might shed light on the folding of chromatin within the physiological setting, where scaffold proteins have long been thought to play a role.

Many chromatin proteins are dynamic, so it would be interesting to see how they localize and function in unfixed, living samples at the scale of chromatin. As our work here reveals, the abundance of contaminating macromolecules within cell extracts poses a serious challenge and fluorescence-based techniques, such as total internal reflection fluorescence microscopy or spinning disk confocal microscopy, may be required if chromatin is to be studied at the single-molecule scale within the cytoplasmic context. Nevertheless, our techniques allow for the rapid isolation of freshly assembled physiological chromatin into buffer, where the chromatin can be manipulated biochemically or supplemented with structural components or enzymes to investigate physiological processes. The major advantage of using cellular extracts is that essential chromatin components can be removed prior to DNA addition without triggering apoptosis, making it possible to study physiological chromatin assembly processes in mutant versus wild-type backgrounds. Future experiments will examine how the absence or overexpression of factors such as histone H1, topoisomerase II, or the condensin complex influences the lower-order structure and morphology of chromatin assembled de novo in egg extract. These factors have been shown to affect chromatin in *Xenopus* egg extracts in previous functional studies, and these can theoretically be applied using our method as well (Hirano and Mitchison 1993; Hirano and Mitchison 1994; Maresca et al. 2005). However, because at the ultrastructural level chromatin shows considerable variability, quantification of these factors' roles will require careful, dedicated studies, and optimization of reaction conditions, and will be based on a combination of both AFM imaging and single-molecule manipulation methods. This work may help bridge the gap between our understanding of simple chromatin arrays in vitro versus the complex and dynamic chromatin structures present in living cells.

Acknowledgments We are grateful to Assistant Professor CA Davey and Ms. MS Ong (Nanyang Technological University) for preparing the reconstituted 12-mer nucleosome array sample, Dr. FM Hameed and Professor GV Shivashankar (Mechanobiology Institute, Singapore) for helping prepare the chromatin sample from live cell nuclei, and Professor JF Marko (Northwestern University) for stimulating discussions. This work was supported by R144000192112 and R144000251112 from the Ministry of Education of Singapore (to JY) and from the Mechanobiology Institute at the National University of Singapore. Work at UC Berkeley was supported by GM057839 to (RH) from The National Institutes of Health.

References

Almouzni G, Wolffe AP (1993) Nuclear assembly, structure, and function: the use of *Xenopus* in vitro systems. Exp Cell Res 205:1–15

Becker PB (2007) Methods in molecular biology—chromatin protocols. Hum Pr 119:509

Bennink ML, Leuba SH, Leno GH, Zlatanova J, de Grooth BG, Greve J (2001) Unfolding individual nucleosomes by stretching single chromatin fibers with optical tweezers. Nat Struct Biol 8:606–610

Cui Y, Bustamante C (2000) Pulling a single chromatin fiber reveals the forces that maintain its higher-order structure. Proc Natl Acad Sci USA 97:127–132

Davey CA, Sargent DF, Luger K, Maeder AW, Richmond TJ (2002) Solvent mediated interactions in the structure of the nucleosome core particle at 1.9 a resolution. J Mol Biol 319:1097–1113

Eltsov M, Maclellan KM, Maeshima K, Frangakis AS, Dubochet J (2008) Analysis of cryo-electron microscopy images does not support the existence of 30-nm chromatin fibers in mitotic chromosomes in situ. Proc Natl Acad Sci U S A 105:19732–19737

Fakan S (2004) The functional architecture of the nucleus as analysed by ultrastructural cytochemistry. Histochem Cell Biol 122:83–93

Fischle W, Tseng BS, Dormann HL, Ueberheide BM, Garcia BA, Shabanowitz J, Hunt DF, Funabiki H, Allis CD (2005) Regulation of HP1-chromatin binding by histone H3 methylation and phosphorylation. Nature 438:1116–1122

Freedman BS, Miller KE, Heald R (2010) *Xenopus* egg extracts increase dynamics of histone H1 on sperm chromatin. PLoS ONE 5:e13111

Hameed FM, Soni GV, Krishnamurthy H, Shivashankar GV (2009) Probing structural stability of chromatin assembly sorted from living cells. Biochem Biophys Res Commun 385:518–522

Hirano T, Mitchison TJ (1991) Cell cycle control of higher-order chromatin assembly around naked DNA in vitro. J Cell Biol 115:1479–1489

Hirano T, Mitchison TJ (1993) Topoisomerase II does not play a scaffolding role in the organization of mitotic chromosomes assembled in *Xenopus* egg extracts. J Cell Biol 120:601–612

Hirano T, Mitchison TJ (1994) A heterodimeric coiled-coil protein required for mitotic chromosome condensation in vitro. Cell 79:449–458

Horowitz-Scherer RA, Woodcock CL (2006) Organization of interphase chromatin. Chromosoma 115:1–14

Horowitz RA, Agard DA, Sedat JW, Woodcock CL (1994) The three-dimensional architecture of chromatin in situ: electron tomography reveals fibers composed of a continuously variable zig-zag nucleosomal ribbon. J Cell Biol 125:1–10

Huynh VA, Robinson PJ, Rhodes D (2005) A method for the in vitro reconstitution of a defined "30 nm" chromatin fibre containing stoichiometric amounts of the linker histone. J Mol Biol 345:957–968

Kireeva N, Lakonishok M, Kireev I, Hirano T, Belmont AS (2004) Visualization of early chromosome condensation: a hierarchical folding, axial glue model of chromosome structure. J Cell Biol 166:775–785

Ladoux B, Quivy JP, Doyle P, du Roure O, Almouzni G, Viovy JL (2000) Fast kinetics of chromatin assembly revealed by single-molecule videomicroscopy and scanning force microscopy. Proc Natl Acad Sci U S A 97:14251–14256

Laskey RA, Mills AD, Morris NR (1977) Assembly of SV40 chromatin in a cell-free system from *Xenopus* eggs. Cell 10:237–243

Losada A, Hirano M, Hirano T (1998) Identification of *Xenopus* SMC protein complexes required for sister chromatid cohesion. Genes Dev 12:1986–1997

Luger K, Mader AW, Richmond RK, Sargent DF, Richmond TJ (1997) Crystal structure of the nucleosome core particle at 2.8 a resolution. Nature 389:251–260

Lusser A, Kadonaga JT (2004) Strategies for the reconstitution of chromatin. Nat Meth 1:19–26

MacCallum DE, Losada A, Kobayashi R, Hirano T (2002) ISWI remodeling complexes in *Xenopus* egg extracts: identification as major chromosomal components that are regulated by INCENP-aurora B. Mol Biol Cell 13:25–39

Maresca TJ, Heald R (2006) Methods for studying spindle assembly and chromosome condensation in *Xenopus* egg extracts. Meth Mol Biol 322:459–474

Maresca TJ, Freedman BS, Heald R (2005) Histone H1 is essential for mitotic chromosome architecture and segregation in *Xenopus laevis* egg extracts. J Cell Biol 169:859–869

McDowall AW, Smith JM, Dubochet J (1986) Cryo-electron microscopy of vitrified chromosomes in situ. EMBO J 5:1395–1402

Murray A (1991) Cell cycle extracts. In *Xenopus laevis* practical uses in cell and molecular biology. Academic, San Diego, pp 581–605

Noll M (1974) Subunit structure of chromatin. Nature 251:249–251

Paulson JR, Laemmli UK (1977) The structure of histone-depleted metaphase chromosomes. Cell 12:817–828

Robinson PJ, Fairall L, Huynh VA, Rhodes D (2006) EM measurements define the dimensions of the "30-nm" chromatin fiber: evidence for a compact, interdigitated structure. Proc Natl Acad Sci U S A 103:6506–6511

Ruberti I, Worcel A (1986) Mechanism of chromatin assembly in *Xenopus* oocytes. J Mol Biol 189:457–476

Sandaltzopoulos R, Becker PB (1999) A solid-phase approach for the analysis of reconstituted chromatin. Meth Mol Biol 119:195–206

Thoma F, Koller T (1977) Influence of histone H1 on chromatin structure. Cell 12:101–107

Thoma F, Koller T, Klug A (1979) Involvement of histone H1 in the organization of the nucleosome and of the salt-dependent super-structures of chromatin. J Cell Biol 83:403–427

Wang H, Bash R, Yodh JG, Hager GL, Lohr D, Lindsay SM (2002) Glutaraldehyde modified mica: a new surface for atomic force microscopy of chromatin. Biophys J 83:3619–3625

Wignall SM, Deehan R, Maresca TJ, Heald R (2003) The condensin complex is required for proper spindle assembly and chromosome segregation in *Xenopus* egg extracts. J Cell Biol 161:1041–1051

Woodcock CL (1994) Chromatin fibers observed in situ in frozen hydrated sections Native fiber diameter is not correlated with nucleosome repeat length. J Cell Biol 125:11–19

Woodcock CL, Ghosh RP (2010) Chromatin higher-order structure and dynamics. Cold Spring Harb Perspect Biol 2: a000596

Yan J, Maresca TJ, Skoko D, Adams CD, Xiao B, Christensen MO, Heald R, Marko JF (2007) Micromanipulation studies of chromatin fibers in *Xenopus* egg extracts reveal ATP-dependent chromatin assembly dynamics. Mol Biol Cell 18:464–474

Zheng C, Lu X, Hansen JC, Hayes JJ (2005) Salt-dependent intra- and internucleosomal interactions of the H3 tail domain in a model oligonucleosomal array. J Biol Chem 280:33552–33557